

**ANTIHYPERTENSIVE AND VASODILATORY  
EFFECTS OF *VERNONIA AMYGDALINA* AND  
*SWIETENIA MACROPHYLLA* EXTRACTS**

**CH'NG YUNG SING**

**UNIVERSITI SAINS MALAYSIA**

**2017**

**ANTIHYPERTENSIVE AND VASODILATORY  
EFFECTS OF *VERNONIA AMYGDALINA* AND  
*SWIETENIA MACROPHYLLA* EXTRACTS**

by

**CH'NG YUNG SING**

**Thesis submitted in fulfillment of the requirements**

**for the degree of**

**Master of Science (Pharmacology)**

**November 2017**

## ACKNOWLEDGEMENT

First and foremost, I would like to express my gratitude to my supervisor, Dr. Yam Mun Fei, for giving me this golden opportunity to conduct my research exercise under his guidance. He led me to the research world, taught me about the mechanisms involved in regulating the blood vessel, opened my mind about the Malaysian local herbs, and accompanied me to Tsinghua University, Beijing to learn the tri-step FTIR analysis method from Professor Sun Su Qin. He taught me something that is more valuable than knowledge, which is our own attitude. He strictly emphasised on the importance of accuracy and consistency of the results. I would also like to thank my co-supervisors Professor Mohd. Zaini Asmawi and Madam Mariam Ahmad for their continuous support and guidance throughout my research work. Next, I would like to thank my lab mate, Tan Chu Shan, Loh Yean Chun, Ng Chiew Hoong, and Yeap Zhao Qin for helping me identify the problems and figuring out the solutions when I faced obstacles in my research.

Besides, I am grateful to the Institute of Postgraduate Studies, Universiti Sains Malaysia for granting me fellowship and supporting me financially which helped me in concentrating on my work and inspired me to work harder. Also, I wish to express my sincere thanks to all the lab technicians for their technical guidance and for training me on handling instruments. Furthermore, my deepest appreciation towards my family and friends that have been my greatest pillar of support. Without them, I would not be able to pull through the entire period of the research.

Last but not least, I would like to acknowledge the lives of the rats that were sacrificed for the sake of the betterment of human. Without the sacrifices of the rats, it is impossible for me to collect these data and significant findings. Finally, those

who have helped me and made sacrifices for me will be remembered for the rest of my life.

## **TABLES OF CONTENTS**

Acknowledgement	ii
Tables of Contents	iv
List of Tables	ix
List of Figures	x
List of Abbreviations	xii
List of Symbols	xviii
Abstrak	xix
Abstract	xxi

### **CHAPTER 1 – INTRODUCTION**

1.1	Hypertension	1
1.2	Herbal remedies in Malaysia	3
1.3	Signaling mechanisms involved in vasorelaxation study	6
1.3.1	cGMP-coupled signal transduction	7
1.3.2	G-protein coupled signal transduction	8
1.3.3	Calcium channels	10
1.3.4	Potassium channels	10
1.4	Problem statement	13
1.5	Objectives	14

### **CHAPTER 2 – TRI-STEP FTIR ANALYSIS OF RAW HERBS**

2.1	Introduction	15
2.2	Materials and methods	17

2.2.1	Materials	17
2.2.2	Biological identification of herbs	17
2.2.3	Tri-step FTIR identification method	18
2.3	Results and discussion	19
2.3.1	Assignments and comparison by using conventional FTIR spectra	19
2.3.2	Comparison and discussion of the SD-IR spectra	24
2.3.3	Comparison and discussion of the 2D-IR spectra	27
2.4	Conclusion	31

### **CHAPTER 3 – VASORELAXATION SCREENING OF EIGHT HERBAL EXTRACTS**

3.1	Introduction	32
3.2	Materials and methods	33
3.2.1	Materials	33
3.2.2	Extraction	34
3.2.3	Experimental animals	34
3.2.4	Preparation of extracts	35
3.2.5	Preparation of isolated rat thoracic aorta <i>in vitro</i>	35
3.2.6	Statistical analysis	36
3.3	Results	37
3.4	Discussion	40
3.5	Conclusion	41

# **CHAPTER 4 – SIGNAL TRANSDUCTION PATHWAYS OF VERNONIA AMYGDALINA ETHANOL EXTRACT IN VASORELAXATION**

4.1	Introduction	42
4.2	Materials and methods	43
4.2.1	Materials	43
4.2.2	Experimental animals	44
4.2.3	Fingerprint analysis by tri-step FTIR spectroscopy	44
4.2.4	Preparation of blockers and extract	44
4.2.5	Aortic ring preparation	45
4.2.6	Determination of the effects of VAE on cGMP-coupled signal transduction and PGI <sub>2</sub> signaling pathway	46
4.2.7	Determination of the roles of VAE on muscarinic and β <sub>2</sub> -adrenergic receptors	46
4.2.8	Determination of the effects of VAE on potassium channels	47
4.2.9	Determination of the effects of VAE on calcium-induced vasoconstriction	47
4.2.10	Determination of the effects of VAE on intracellular Ca <sup>2+</sup> release from sarcoplasmic reticulum	48
4.2.11	Statistical analysis	48
4.3	Results	48
4.3.1	Tri-step FTIR macro-fingerprint of VAE	48
4.3.2	Effects of VAE on PE pre-contracted aortic rings	52
4.3.3	Roles of VAE on endothelium-dependent vasorelaxant factors	54
4.3.4	Endothelium-independent mechanisms of VAE	54
4.3.5	Roles of VAE on potassium channels	57

4.3.6	Roles of VAE on calcium channels	60
4.4	Discussion	63
4.4.1	Assignments of tri-step FTIR macro-fingerprint of VAE	63
4.4.2	Possible vasorelaxant mechanisms of VAE	65
4.5	Conclusion	70

## **CHAPTER 5 – SIGNAL TRANSDUCTION PATHWAYS OF 50% ETHANOL EXTRACT OF *SWIETENIA MACROPHYLLA* SEEDS IN VASORELAXATION**

5.1	Introduction	72
5.2	Materials and methods	73
5.3	Results	74
5.3.1	Tri-step FTIR macro-fingerprint of SM50	74
5.3.2	Vasorelaxant effects of SM50 on PE pre-contracted aortic rings	78
5.3.3	Roles of SM50 on endothelium-dependent vasorelaxant factors	80
5.3.4	Endothelium-independent mechanisms of SM50	83
5.3.5	Roles of SM50 on potassium channels	83
5.3.6	Roles of SM50 on calcium channels	87
5.4	Discussion	91
5.4.1	Assignments of tri-step FTIR macro-fingerprint of SM50	91
5.4.2	Possible vasorelaxant mechanisms of SM50	92
5.5	Conclusion	98



**CHAPTER 6 – ANTIHYPERTENSIVE EFFECT AND SUB-ACUTE  
TOXICITY STUDIES OF 50% ETHANOL EXTRACT  
OF *SWIETENIA MACROPHYLLA* SEEDS**

6.1	Introduction	99
6.2	Materials and methods	100
6.2.1	Materials	100
6.2.2	Animal models	100
6.2.3	Antihypertensive study of SM50	100
6.2.4	Sub-acute toxicity study	101
6.2.5	Statistical analysis	103
6.3	Results	103
6.3.1	SM50 attenuates the blood pressure of SHR	103
6.3.2	Sub-acute toxicity, body weight, and relative organ weight	105
6.3.3	Hematology and blood biochemistry	108
6.4	Discussion	111
6.5	Conclusion	114

**CHAPTER 7 - CONCLUSION** 116

**REFERENCES** 118

**APPENDICES**

**LIST OF PUBLICATIONS**

## LIST OF TABLES

	<b>Page</b>
Table 1.1    Classification of blood pressure	2
Table 2.1    Peak assignments on the conventional FTIR spectra of herbs	23
Table 3.1    Yield of herbal extracts	38
Table 3.2    Vasorelaxation screening of different herbal extracts on pre-contracted aortic rings	39
Table 4.1    Peak assignments on the FTIR spectrum of VAE	51
Table 4.2    Values of the EC <sub>50</sub> and maximum relaxation (R <sub>max</sub> ) response of VAE in isolated rat aortic rings pre-treated with various antagonists	59
Table 5.1    Peak assignments on the conventional FTIR spectrum of SM50	77
Table 5.2    Values of EC <sub>50</sub> and maximum relaxation (R <sub>max</sub> ) response on SM50-induced vasorelaxation to different antagonists	86
Table 6.1    Relative organ weight of SHR after four weeks of study	107
Table 6.2    Hematology values of SHR after four weeks of study	109
Table 6.3    Biochemical parameters of SHR after four weeks of study	110

## LIST OF FIGURES

		Page
Figure 1.1	Pictures of (a) <i>C. nutans</i> , (b) <i>S. cripus</i> , (c) <i>M. bacteata</i> , (d) <i>E. scaber</i> , (e) <i>P. bleo</i> , (f) <i>P. grandifolia</i> , (g) <i>V. amygdalina</i> , and (h) <i>S. macrophylla</i> .	4
Figure 1.2	Signaling pathways involved in vascular tone regulation.	12
Figure 2.1	Conventional FTIR spectra of (a) <i>C. nutans</i> , (b) <i>S. cripus</i> , (c) <i>M. bacteata</i> , (d) <i>E. scaber</i> , (e) <i>P. bleo</i> , (f) <i>P. grandifolia</i> , (g) <i>V. amygdalina</i> , and (h) <i>S. macrophylla</i> seed.	22
Figure 2.2	SD-IR spectra of (a) <i>C. nutans</i> , (b) <i>S. cripus</i> , (c) <i>M. bacteata</i> , (d) <i>E. scaber</i> , (e) <i>P. bleo</i> , (f) <i>P. grandifolia</i> , (g) <i>V. amygdalina</i> , and (h) <i>S. macrophylla</i> seed in the range of 1800 – 800 cm <sup>-1</sup> .	26
Figure 2.3	The 2D-IR fingerprints of (a) <i>C. nutans</i> , (b) <i>S. cripus</i> , (c) <i>M. bacteata</i> , (d) <i>E. scaber</i> , (e) <i>P. bleo</i> , (f) <i>P. grandifolia</i> , (g) <i>V. amygdalina</i> , and (h) <i>S. macrophylla</i> seed in the range of 1200 – 1800 cm <sup>-1</sup> .	30
Figure 4.1	Fingerprint of VAE in (a) conventional FTIR, (b) second derivative in the range of 1800 – 700 cm <sup>-1</sup> and (c) 2D-IR spectra in the range of 1200 – 1800 cm <sup>-1</sup> .	50
Figure 4.2	Effect of VAE on PE-induced contraction in endothelium-intact aortic rings and endothelium-denuded aortic rings (n = 8).	53
Figure 4.3	Effect of VAE on PE-induced contraction in endothelium-intact aortic rings (n = 8) in the presence of L-NAME, indomethacin and atropine.	55
Figure 4.4	Effect of propranolol, MB, and ODQ on the vasorelaxant effect of VAE in endothelium-intact aortic rings (n = 8) pre-contracted by PE.	56
Figure 4.5	Effect of VAE on PE-induced contraction in endothelium-intact aortic rings (n = 8) in the presence of TEA, glibenclamide, 4-AP and BaCl <sub>2</sub> .	58
Figure 4.6	Effect of VAE on CaCl <sub>2</sub> -induced vasocontraction in isolated aortic rings (n = 8).	61
Figure 4.7	Vasorelaxant effect of VAE on PE pre-contracted endothelium-denuded aortic rings in Ca <sup>2+</sup> -free Krebs' solution (n = 8).	62

Figure 5.1	Fingerprint of SM50 in (a) conventional FTIR, (b) second derivative in the range of 1800 – 800 cm <sup>-1</sup> , and (c) 2D-IR spectra in the range of 1000 – 1750 cm <sup>-1</sup> .	76
Figure 5.2	Effect of SM50 on PE-induced contraction in endothelium-intact aortic rings and endothelium-denuded aortic rings (n = 8).	79
Figure 5.3	Effect of SM50 on PE-induced contraction in endothelium-intact aortic rings (n = 8) in the presence of L-NAME, ODQ, MB, and indomethacin.	81
Figure 5.4	Effect of atropine on the vasorelaxant effect of SM50 on endothelium-intact aortic rings (n = 8) pre-contracted with PE.	82
Figure 5.5	Effect of propranolol on the vasorelaxant effect of SM50 in endothelium-intact aortic rings pre-contracted with PE.	84
Figure 5.6	Effect of SM50 on PE-induced contraction in endothelium-intact aortic ring in the presence of TEA, 4-AP, BaCl <sub>2</sub> , and glibenclamide.	85
Figure 5.7	Effect of SM50 on CaCl <sub>2</sub> -induced vasocontraction in isolated aortic rings (n = 8).	89
Figure 5.8	Vasorelaxant effect of SM50 mediated by intracellular release of calcium (n = 8).	90
Figure 6.1	Effect of three different dose of SM50 on (a) SBP, (b) DBP, and (c) MAP in SHR (n = 6).	104
Figure 6.2	Body weight of SHR during four weeks of study (n = 6).	106

## LIST OF ABBREVIATIONS

2-APB	2-aminoethoxydiphenyl borate
2D-IR	Two-dimensional correlation infrared
4-AP	4-aminopyridine
5-HT	Serotonin
AA	Arachidonic acid
AC	Adenylyl cyclase
ACEIs	Angiotensin-converting enzyme inhibitors
ACh	Acetylcholine
A/G	Albumin/globulin
ALP	Alkaline phosphatase
ALT	Alanine aminotransferase
ANOVA	Analysis of variance
ARBs	Angiotensin receptor blockers
AST	Aspartate aminotransferase
AT	Angiotensin
ATP	Adenosine triphosphate
B <sub>2</sub>	Bradykinin
BaCl <sub>2</sub>	Barium chloride
BK <sub>Ca</sub>	Big-conductance calcium-activated potassium channel
Ca <sup>2+</sup>	Calcium ion
CaCl <sub>2</sub>	Calcium chloride
cAMP	Cyclic adenosine monophosphate
CBC	Complete blood count
CCBs	Calcium channel blockers

CE	Capillary electrophoresis
cGMP	Cyclic guanosine monophosphate
CMC	Carboxymethyl cellulose
CO <sub>2</sub>	Carbon dioxide
COX	Cyclooxygenase
DAG	Diacylglycerol
DBil	Direct bilirubin
DBP	Diastolic blood pressure
DNA	Deoxyribonucleic acid
DRI	Direct rennin inhibitor
DTGS	Deuterated Tri-Glycine Sulfate
EC <sub>50</sub>	Median effective concentration
EDHF	Endothelium-derived hyperpolarizing factor
EDRFs	Endothelium-dependent relaxing factors
EDTA	Ethylenediaminetetraacetic acid
EGTA	Ethylene glycol tetraacetic acid
eNOS	Endothelial nitric oxide synthase
ET	Endothelin
FTIR	Fourier transform infrared
GC	Gas chromatography
GGT	Gamma-glutamyl transferase
GI	Gastrointestinal
GPCR	G-protein-coupled receptor
GTP	Guanosine triphosphate
HCT	Hematocrit

HGB	Hemoglobin
HPLC	High performance liquid chromatography
IBil	Indirect bilirubin
IK <sub>Ca</sub>	Intermediate-conductance calcium-activated potassium channel
IP	Prostaglandin I <sub>2</sub>
IP <sub>3</sub>	Inositol trisphosphate
IP <sub>3</sub> R	Inositol trisphosphate receptor
IR	Infrared
K <sup>+</sup>	Potassium ion
K <sub>ATP</sub>	ATP-sensitive potassium channels
K <sub>Ca</sub>	Calcium-activated potassium channels
K <sub>IR</sub>	Inwardly rectifying potassium channels
K <sub>V</sub>	Voltage-dependent potassium channels
KBr	Potassium bromide
KCl	Potassium chloride
Krebs'	Krebs-Henseleit
L-NAME	L-N <sup>G</sup> -Nitroarginine methyl ester
L-NNA	N $\omega$ -nitro-L-arginine
LC/MS	Liquid chromatography with mass spectrometry
LD <sub>50</sub>	Median lethal dose
LDCC	Ligand-dependent calcium channel
LFT	Liver function test
M <sub>3</sub>	Muscarinic
MAP	Mean arterial pressure
MB	Methylene blue

MCH	Mean cell hemoglobin
MCHC	Mean cell hemoglobin concentration
MCV	Mean corpuscular volume
Mg <sup>2+</sup>	Magnesium ion
MgSO <sub>4</sub>	Magnesium sulfate
MLC	Myosin light chain
MLCK	Myosin light chain kinase
MLCP	Myosin light chain phosphate
n	Number of determination
NaCl	Sodium chloride
NaHCO <sub>3</sub>	Sodium bicarbonate
NaH <sub>2</sub> PO <sub>4</sub>	Sodium dihydrogen phosphate
NO	Nitric oxide
NO-cGMP	Nitric oxide-cyclic guanosine monophosphate
NSAIDs	Non-steroidal anti-inflammatory drugs
O <sub>2</sub>	Oxygen
ODQ	1H-(1,2,4)Oxadiazolo(4,3-a)quinoxalin-1-one
PE	Phenylephrine
PGI <sub>2</sub>	Prostacyclin
PIP <sub>2</sub>	Phosphatidylinositol 4,5-bisphosphate
PKC	Protein kinase C
PKG	cGMP-dependent protein kinase
PLC	Phospholipase C
PLT	Platelet
R <sub>max</sub>	Maximum relaxation



RBC	Red blood cell
RFT	Renal function test
ROCC	Receptor-operated calcium channel
RyR	Ryanodine receptor
SBP	Systolic blood pressure
SD	Sprague-Dawley
SD-IR	Second derivative infrared
SEM	Standard error of mean
SERCA	sarco/endoplasmic reticulum $\text{Ca}^{2+}$ -ATPase
sGC	Soluble guanylyl cyclase
SHRs	Spontaneously hypertensive rats
$\text{SK}_{\text{Ca}}$	Small-conductance calcium-activated potassium channel
SM50	50% ethanol extract of <i>S. macrophylla</i> seed
SOCC	Store-operated calcium channel
SPSS	Statistical Package for Social Sciences
SR	Sarcoplasmic reticulum
TBil	Total bilirubin
TEA	Tetraethylammonium ion
TLC	Thin layer chromatography
TP	Total protein
TSMs	Traditional Systems of Medicine
$\text{TxA}_2$	Thromboxane
UK	United Kingdom
USA	United States of America
USM	Universiti Sains Malaysia

UV	Ultraviolet
VAE	<i>V. amygdalina</i> 95% ethanol extract
VOCC	Voltage-operated calcium channel
VSM	Vascular smooth muscle
VSMCs	Vascular smooth muscle cells
WBC	White blood cell

## LIST OF SYMBOLS

%	Percentage
°C	Degree Celsius
°C/min	Degree Celsius per minute
10 <sup>9</sup> /L	10 <sup>9</sup> cells per liter
10 <sup>12</sup> /L	10 <sup>12</sup> cells per liter
μL	Microliter
μM	Micromolar
μmol/L	Micromole per liter
cm <sup>-1</sup>	Reciprocal centimeter
fL	Femtoliter
g	Gram
g/dL	Gram per deciliter
g/L	Gram per liter
h	Hour
mg	Milligram
mg/mL	Milligram per milliliter
min	Minute
mM	Millimolar
mm	Millimeter
mmHg	Millimeter of mercury
mmol/L	Millimole per liter
pg	Picogram
rpm	Revolution per minute
U/L	Units per liter

# KESAN ANTIHIPERTENSI DAN VASODILATORI EKSTRAK *VERNONIA* *AMYGDALINA* DAN *SWIETENIA MACROPHYLLA*

## ABSTRAK

Di Malaysia, hipertensi merupakan topik hangat dalam kesihatan awam dan perubatan, oleh demikian, cara penyelesaian amat diperlukan. Dalam kajian ini, herba tempatan Malaysia seperti *Clinacanthus nutans* Lindau, *Strobilanthes crispus*, *Murdannia bacteata*, *Elephantopus scaber* Linn., *Pereskia bleo*, *Pereskia grandifolia* Haw., *Vernonia amygdalina*, dan benih *Swietenia macrophylla* King telah dipilih dan ekstraknya (ekstrak air, ekstrak 50% etanol, dan ekstrak 95% etanol) telah digunakan untuk kajian permulaan awal bagi aktiviti antihipertensi dan pemvasokenduran. Keputusan menunjukkan bahawa benih *Swietenia macrophylla* King mempunyai potensi tertinggi dalam pemvasokenduran, diikuti oleh *Vernonia amygdalina*. Oleh itu, ekstrak 95% etanol daripada *V. amygdalina* (VAE) dan ekstrak 50% etanol daripada benih *S. macrophylla* King (SM50) yang menunjukkan potensi terbaik dalam pemvasokenduran telah disiasat selanjutnya mekanisme tindakan pemvasokenduran melalui kajian *in vitro* dengan merakam tindak balas kontraksi cincin aorta yang terpencil terhadap ekstrak dengan kehadiran penyekat tertentu. Kajian telah menunjukkan VAE dan SM50 yang mengandungi kepelbagaian komponen kimia menunjuk kesan pemvasokenduran yang lebih kuat ke atas cincin aorta kerana mungkin melibatkan pelbagai mekanisme. Laluan utama yang menyebabkan kesan pemvasokenduran oleh VAE dalam *in vitro* cincin aorta terpencil adalah melalui EDRF yang merangkumi PGI<sub>2</sub> dan NO, diikuti oleh reseptor saluran berpaut (sebagai pembuka saluran K<sup>+</sup>), dan seterusnya faktor relaksasi tanpa-

endotelium seperti laluan isyarat reseptor- $M_3$  dan  $\beta_2$ . Manakala laluan pemvasokonduran SM50 kebanyakannya melibatkan laluan reseptor saluran berpaut (penyumbatan VOCC, pembuka saluran  $K^+$  dan penghambat reseptor  $IP_3$ ) dan kurang terlibat dalam laluan  $\beta_2$ -adrenergik tanpa-endotelium dan laluan isyarat NO/sGC/cGMP. Selain itu, SM50 juga digunakan dalam kajian *in vivo* ke atas spontaneously hypertensive rats (SHRs) melalui penyusunan tiga dos SM50 yang berbeza (1000 mg/kg, 500 mg/kg dan 250 mg/kg) dengan intubasi gastrik sekali setiap hari selama empat minggu. Setelah empat minggu rawatan, penurunan nilai SBP, DBP, dan MAP yang ketara dapat dilihat dalam ketiga-tiga kumpulan SHRs dan tindak balas antihipertensi telah muncul walaupun hanya selepas minggu pertama penyusunan. Ini membuktikan bahawa SM50 mempunyai kesan antihipertensi yang kuat dan aktiviti antihipertensinya adalah bergantung kepada kepekatan ekstrak. Dalam pada itu, kajian toksisiti menunjukkan bahawa SHRs yang dirawat 1000 mg/kg/hari SM50 selama 28 hari telah menunjukkan hepatotoksiti. Ujian fungsi hati menunjukkan peningkatan tahap transferas gama-glutamil (GGT) yang ketara ( $35.00 \pm 10.61$  U/L) dan pengurangan yang ketara untuk tahap albumin ( $9.70 \pm 0.72$  g/L). SHRs juga mengalami penurunan berat badan (9.47% untuk 1000 mg/kg, 5.15% untuk 500 mg/kg, dan 7.46% untuk 250 mg/kg). Oleh itu, dapat disimpulkan bahawa SM50 mungkin menyebabkan hepatotoksik pada 1000 mg/kg dan dos yang selamat untuk tikus adalah disyorkan pada sekitar 250 mg/kg. Walau bagaimanapun, masih terlalu awal untuk menyimpulkan bahawa dos ini adalah selamat untuk digunakan pada manusia, lebih banyak kajian harus dijalankan sebelum membuat kesimpulan yang kukuh.

**ANTIHYPERTENSIVE AND VASODILATORY EFFECTS OF *VERNONIA*  
*AMYGDALINA* AND *SWIETENIA MACROPHYLLA* EXTRACTS**

**ABSTRACT**

In Malaysia, hypertension is an increasingly important medical and public health issue and there is an imminent need to decrease its prevalence. In this study, the local herbs in Malaysia such as *Clinacanthus nutans* Lindau, *Strobilanthes crispus*, *Murdannia bacteata*, *Elephantopus scaber* Linn., *Pereskia bleo*, *Pereskia grandifolia* Haw., *Vernonia amygdalina*, and *Swietenia macrophylla* King seeds were selected and their extracts (water extracts, 50% ethanol extracts, and 95 % ethanol extracts) underwent preliminary testing to screen for their antihypertensive activities and their vasorelaxation. The results showed that the seeds of *Swietenia macrophylla* King has the highest potential in vasorelaxation, followed by *Vernonia amygdalina*. Thus, the vasorelaxation mechanism of *V. amygdalina* and *S. macrophylla* seeds extracts with the best potential in vasorelaxation (95% ethanol extract of *V. amygdalina*, VAE and 50% ethanol extract of *S. macrophylla* seeds, SM50) were further investigated through *in vitro* study by recording the contractile responses of the isolated aortic rings to the extracts with the presence of selective blockers. This study found that, crude VAE and SM50, which contain multiple chemical components, exhibited a stronger vasorelaxant effect on isolated aortic rings due to their possible involvement of multiple mechanisms. The major route for inducing the vasorelaxant effect by VAE in *in vitro* isolated aortic rings was via EDRFs which includes PGI<sub>2</sub> and NO, followed by channel-linked receptors (as K<sup>+</sup> channels opener), and subsequently endothelium-independent relaxing factors such as M<sub>3</sub>- and β<sub>2</sub>-receptors signaling

pathways. While the vasorelaxation pathways employed by SM50 were mostly attributed to channel-linked receptors pathways (blockage of VOCC, K<sup>+</sup> channels opener, and IP<sub>3</sub> receptor inhibitor), with smaller contributions from the endothelium-independent  $\beta_2$ -adrenergic pathways, and the NO/sGC/cGMP signalling pathways. Besides, SM50 also underwent an *in vivo* study through orally administered spontaneously hypertensive rats (SHRs) with three different doses of SM50 (1000 mg/kg, 500 mg/kg, and 250 mg/kg) by gastric intubation once a day for four weeks. After four weeks of treatment, a clear decrease in the SBP, DBP, and MAP values could be observed in the three groups of SHRs and it only took one week for the antihypertensive action to manifest. This indicated that SM50 possess strong antihypertensive effect and its antihypertensive activity is strongly concentration dependent. However, toxicity study showed that SHRs which were treated with 1000 mg/kg/days of SM50 for 28 days exhibited hepatotoxicity. The liver function tests showed significant elevation of gamma-glutamyl transferase (GGT) level ( $35.00 \pm 10.61$  U/L) and significant reduction in albumin level ( $9.70 \pm 0.72$  g/L). The SHRs also experienced decrease in body weights (9.47% for 1000 mg/kg, 5.15% for 500 mg/kg, and 7.46% for 250 mg/kg). Therefore, it can be concluded that SM50 might cause hepatotoxic effect at 1000 mg/kg and the suggested safety doses for rat is 250 mg/kg. However, it is too early to conclude that this dosage is safe for consumption in human, more studies should be conducted before drawing a firm conclusion.

## CHAPTER 1

### INTRODUCTION

#### 1.1 Hypertension

Hypertension is a chronic medical condition in which the blood pressure is elevated (a sustained systolic blood pressure greater than 140 mmHg and/or a sustained diastolic blood pressure greater than 90 mmHg). This may lead to stroke, heart disease, and heart failure. Besides, the other organs such as kidneys, limbs, and eyes may also suffer damage. Typically, hypertension has been classified into four classes (see Table 1.1) by the seventh report of Joint National Committee (Lenfant et al., 2003). In Malaysia, hypertension is an increasingly important medical and public health issue. According to Hypertension Clinical Practice Guidelines of Malaysia on 2013, the prevalence of hypertension in Malaysia for adults of more than 18 years old has increased from 32.2% in 2006 to 32.7% in 2011, whereas for those adults of more than 30 years old, the prevalence has increased from 42.6% to 43.5%. Therefore, there is an imminent need to decrease the prevalence of hypertension.

It is known that lowering blood pressure can greatly reduce hypertension complication such as cerebrovascular, cardiovascular, and renal disease (Wang et al., 2014). An impressive evolution of antihypertensive agents have been developed over the few past decades. In early, a *Rauwolfia* alkaloids, reserpine was widely used as antihypertensive drugs, however it has been replaced by other drugs due to its drastic side effects including depression and cancer (Lobay, 2015). In 1950s, thiazide diuretics had discovered helpful in lowering blood pressure, followed by  $\beta$ -blockers, calcium channel blockers (CCBs),  $\alpha$ -blockers, angiotensin-converting enzyme



inhibitors (ACEIs), angiotensin receptor blockers (ARBs), and direct renin inhibitor (DRI) Aliskiren in subsequent years for antihypertensive drugs development (Düsing, 2010). However, there are five of the aforementioned antihypertensive drugs (thiazide diuretics,  $\beta$ -blockers, CCBs, ACEIs, and ARBs) have been stated in the Clinical Practice Guidelines in Management of Hypertension as the current most frequently choices of first line mono-therapy drugs for treating hypertension. Nonetheless, combination drugs often being preferred since they exert a better antihypertensive effect compared to single drug therapy (MOH, 2013). At this point, crude extract of local herbs could achieve the holistic therapeutic criteria whereby treating the hypertension by using multiple signaling mechanism pathways instead of either one of the mono-pathway. Native plant remedies are readily available, low cost and are less likely to cause safety concern (Taiwo et al., 2010). Therefore, awareness about its importance in health care delivery system is growing tremendously. These benefits also reinforces the use of local herbs in this current study.

**Table 1.1** Classification of blood pressure

<b>Classification</b>	<b>Systolic Blood Pressure (mmHg)</b>	<b>Diastolic Blood Pressure (mmHg)</b>
Normal	$\leq 120$	$\leq 80$
Prehypertension	120 – 139	80 – 89
Stage 1 hypertension	140 – 159	90 – 99
Stage 2 hypertension	$\geq 160$	$\geq 100$

## 1.2 Herbal remedies in Malaysia

In Traditional Systems of Medicine (TSMs), medicines from natural origin have been used as a source of remedy for the prevention, cure, and treatment of different ailments (Rates, 2001). Herbal medicine has always been an asset to the people of Malaysia due to our country's rich herbal resources. Therapeutically important plants in TSMs have been extensively explored recently, for their benefits and various applications in herbal health supplements (Borris, 1996, Gurib-Fakim, 2006, Katiyar et al., 2012). Furthermore, traditional medicine strategy published recently states that traditional and complementary medicines have gained a growing economic importance worldwide (Qi and Kelley, 2014). Therefore, bringing the consumption and use of such remedies into a valid framework for the rational scientific use of such medicines is imperative.

Malaysia is a tropical country with plentiful rainforests, a lot of herbs could grow throughout the year. Most of the local herbs in Malaysia such as *Clinacanthus nutans* Lindau, *Strobilanthes crispus*, *Murdannia bacteata*, *Elephantopus scaber* Linn., *Pereskia bleo*, *Pereskia grandifolia* Haw., *Vernonia amygdalina*, and *Swietenia macrophylla* King (Figure 1.1) are widely distributed plants used for dietary and medicinal purposes due to they are safe to consume and less information showed they are toxic (Chen et al., 2010, Goh, 2000, Quasie et al., 2016, Tan et al., 2005).



(a)



(b)



(c)



(d)



(e)



(f)



(g)



(h)

**Figure 1.1** Pictures of (a) *C. nutans*, (b) *S. crispus*, (c) *M. bacteata*, (d) *E. scaber*, (e) *P. bleo*, (f) *P. grandifolia*, (g) *V. amygdalina*, and (h) *S. macrophylla*.

According to Goh (2001), *Clinacanthus nutans* Lindau, *Strobilanthes cripus*, *Murdannia bacteata*, *Elephantopus scaber* Linn., *Pereskia bleo*, *Pereskia grandifolia* Haw., *Vernonia amygdalina*, and *Swietenia macrophylla* King are traditionally used in Malaysia to treat cancer, inflammation, diabetes, hypertension, and act as antioxidant agents.

Their uses in traditional medicine have been scientifically supported by numerous studies. For example, *Clinacanthus nutans* Lindau has been reported to possess antioxidant, anti-inflammation, antimicrobial, and anti-viral activity (Mustapa et al., 2015, P'ng et al., 2013). Preclinical studies have shown that the *Strobilanthes cripus* possess antioxidant, free radical-scavenging, anticancer, antidiabetic, antimicrobial, wound healing, and antiulcerogenic activities (Nurraihana and Norfarizan-Hanoon, 2013). The extracts of *Murdannia bracteata* have been reported to have hepatoprotective effects and antioxidant activity (Ooi et al., 2015, Yam et al., 2010). The whole plant of *Elephantopus scaber* Linn. had been tested for acute toxicity, and has analgesic, antipyretic, antimicrobial, antioxidant, antidiabetic, anti-inflammatory, cardiovascular, hepatoprotective, diuretic, and laxative activities (Hiradeve and Rangari, 2014, Poli et al., 1992). There are several pharmacological reports on the extracts of *Pereskia bleo*, mainly on cytotoxic, anti-proliferative and anti-nociceptive activities (Abdul-Wahab et al., 2012, Sri Nurestri et al., 2008). Some experimental pharmacological studies with *Pereskia grandifolia* Haw. have reported the anti-tumor, antioxidant potential, diuretic activity, and hypotensive effect its extracts (Kazama et al., 2012, Nurestri et al., 2009, Sim et al., 2010). A number of studies have shown that *Vernonia amygdalina* possesses antioxidant, anti-hyperlipidemic, and antidiabetic properties (Adaramoye et al., 2008, Akah and Okafor, 1992, Atangwho et al., 2013, Ijeh and Ejike, 2011). Based on the previous

research, various pharmacological activities of *Swietenia macrophylla* King leaves had been established, which include antimicrobial, anti-inflammatory, antioxidant effects, anticancer, antitumor, and anti-diabetic activities (Moghadamtousi et al., 2013), while the seeds of *Swietenia macrophylla* King have the effect against hypertension and diabetes (Ch'ng et al., 2016, Hashim et al., 2013).

The knowledge of using the above mentioned herbal remedies to treat hypertension had been passed down for generations. However, these concepts have yet to be proven scientifically and there was no evidence to prove that these herbs possess antihypertensive activity. Thus, it is important to do a preliminary test to screen for the antihypertensive activities of these herbs.

### **1.3 Signaling mechanisms involved in vasorelaxation study**

Blood vessels isolated from living organisms are commonly used for the *in vitro* studies on anti-hypertensive drugs research (Yildiz et al., 2013). Blood pressure are regulated within a narrow range where the blood could convey sufficient perfusion for tissue but not cause any harm on the vascular system, especially the endothelium and vascular smooth muscle cells (Loh et al., 2016). Therefore, it is important to study and focus on the signaling mechanism pathways involved in vascular tone regulation to keep the blood pressure in the optimal range, including signaling amplification from second messengers and the interaction between enzyme-linked, channel-linked and G-protein coupled receptors.

There are several signal transduction mechanisms that modulate intracellular calcium concentration and so for the vascular tone. The primary pathways involved in the vasorelaxation of blood vessels are nitric oxide-cyclic guanosine

monophosphate (NO-cGMP) pathway and G-protein-coupled pathway. They are subsequently followed by the potassium channels, which can be subdivided into calcium-activated potassium channels ( $K_{Ca}$ ), ATP-sensitive potassium channels ( $K_{ATP}$ ), voltage-dependent potassium channels ( $K_V$ ), and inwardly rectifying potassium channels ( $K_{IR}$ ). Calcium channels are essentially involved in the regulation of vascular tone and they are also divided into a few groups, such as voltage-operated calcium channel (VOCC), receptor-operated calcium channel (ROCC), store-operated calcium channel (SOCC), as well as the sarco/endoplasmic reticulum  $Ca^{2+}$ -ATPase (SERCA) signaling pathways (Loh et al., 2016).

### **1.3.1 cGMP-coupled signal transduction**

NO-cGMP system is very important in regulating vascular smooth muscle tone. Vascular endothelial cells normally produce NO by endothelial nitric oxide synthase (eNOS) from the breakdown of L-arginine. NO diffuses from endothelial cells to adjacent vascular smooth muscle cells (VSMCs) where it activates soluble guanylyl cyclase (sGC) leading to increased formation of cGMP second messenger from guanosine triphosphate (GTP) and cause vasorelaxation (Jakala et al., 2009, Moncada, 2007). The cGMP relaxes vascular smooth muscle (VSM) through several ways, such as stimulates cGMP-dependent protein kinase (PKG) that activates myosin light chain phosphate (MLCP) which dephosphorylates myosin light chain (MLC), inhibits calcium entry into the VSM which decreases intracellular calcium concentrations, activates  $K^+$  channels which leads to hyperpolarization, and decreases inositol trisphosphate ( $IP_3$ ) ( Horowitz et al., 1996, Klabunde, 2011, Ko et al., 2008).

### 1.3.2 G-protein coupled signal transduction

G-protein-coupled receptor (GPCR) will responds to ligands through the activation of the G-proteins, which are located on the intracellular surface of the cell membrane. In general, G-protein can be categorized into  $\alpha$ ,  $\beta$ , and  $\gamma$  types. Once GTP is bound to the G-protein and activates it, the G-protein is cleaved into  $G\alpha$  and  $G\beta\gamma$  dimmers. Typically,  $G\alpha$ -proteins can be classified into  $G_s\alpha$ ,  $G_i\alpha$ , and  $G_q\alpha$  which are functionally responsible for different roles in signaling transduction of blood vessels (Walaas et al., 1992).

The  $G_s\alpha$ -protein coupled pathway in VSM stimulates adenylyl cyclase (AC), which catalyses the formation of cyclic adenosine monophosphate (cAMP) second messenger from adenosine triphosphate (ATP) (Berumen et al., 2012, Nichols and Nichols, 2008). An increase in cAMP in VSM causes relaxation or reduced contraction. The reason for this opposite effect is that calcium-calmodulin activates myosin light chain kinase (MLCK), which phosphorylates MLC and causes contraction, however, MLCK is inhibited by cAMP. The  $G_s\alpha$ -protein is coupled to several important receptors that bind vasorelaxant substances, among which are  $\beta_2$ -adrenoceptors (bind to  $\beta_2$ -agonists such as epinephrine and isoproterenol),  $A_2$  purinergic receptors (bind to adenosine), and prostaglandin  $I_2$  (IP) receptors (bind prostacyclin,  $PGI_2$ , which is produced from arachidonic acid, AA and catalysed by cyclooxygenase, COX in endothelial cell) (Bonaventura et al., 2011, Jakala et al., 2009, Klabunde, 2011).

Whereas,  $G_i\alpha$ -protein is functionally opposed to  $G_s\alpha$ -protein.  $G_i\alpha$ -protein in VSM is coupled to  $\alpha_2$ -adrenoceptor. Binding of this receptor to an agonist such as norepinephrine causes a reduction in cAMP, which leads to VSM contraction (Klabunde, 2011, Qin et al., 2008).

In VSMC, there are two signal transduction pathways linked to  $G_q\alpha$ -protein which are phospholipase C (PLC) pathway and Rho-kinase pathway. In PLC pathway, the activated  $G_q\alpha$ -protein stimulates PLC to form  $IP_3$  and diacylglycerol (DAG) from phosphatidylinositol 4,5-bisphosphate ( $PIP_2$ ),  $IP_3$  bound to the  $IP_3$  receptor which located in the membrane of sarcoplasmic reticulum (SR) and stimulates SR release of calcium to the cytoplasm, while DAG activates protein kinase C (PKC) and stimulates contraction. The Rho-kinase pathway inhibits MLCP, which enhances contraction (Jakala et al., 2009, Klabunde, 2011, Yildiz et al., 2013).

Most of the  $G_q\alpha$ -protein-coupled receptors such as angiotensin (AT) receptor, serotonin (5-HT) receptor, muscarinic ( $M_3$ ) receptor, and endothelin (ET) receptor are present in both endothelium and VSMC. However, AT receptor, 5-HT receptor, and ET receptor are functionally predominated in VSMC, while  $M_3$  receptor is functionally predominated in endothelium. In addition of this, the other  $G_q\alpha$ -protein-coupled receptors such as  $\alpha_1$ -adrenergic receptor and thromboxane ( $TxA_2$ ) receptor exist only in VSMC, and bradykinin ( $B_2$ ) receptors exist only in the endothelium. In the endothelium, the  $G_q\alpha$ -protein-coupled receptors produce NO by increasing the intracellular concentration of calcium in endothelium and subsequent eNOS activation. Whereas in the VSMC, the  $G_q\alpha$ -protein-coupled receptors produce a direct effect in the increase of intracellular concentration of calcium by passing through the PLC-dependent pathway (Bockaert et al., 2006, Chen et al., 2000, de Gasparo et al., 2000, Goodman et al., 2001, Ishii and Kurachi, 2006, Jakala et al., 2009, Klabunde, 2011, Loh et al., 2016, Yildiz et al., 2013).



### 1.3.3 Calcium channels

There are two main groups of calcium channels in VSMCs, namely voltage-operated calcium channel (VOCC, also called L-type calcium channels) and ligand-gated calcium channels (such as ROCC and SOCC). IP<sub>3</sub> receptor (IP<sub>3</sub>R) and Ryanodine receptor (RyR) are also classified as ligand-gated calcium channels which locate in the membrane of SR (Landsberg and Yuan, 2004, McFadzean and Gibson, 2002). When an agonist binds to a G<sub>q</sub>α-protein-coupled receptor, it trigger the formation of DAG and IP<sub>3</sub>. DAG activates ROCC mediated calcium influx and IP<sub>3</sub> activates IP<sub>3</sub>R mediated calcium release from SR and cause membrane depolarization (Putney et al., 2001). The subsequent depletion of calcium from SR in turn activates SOCC mediated calcium influx and the membrane depolarization leads to VOCC mediated large amount of calcium influx and cause vasoconstriction (Feletou and Vanhoutte, 2005, McFadzean and Gibson, 2002). The high level of cytoplasmic calcium concentration also triggering RyR mediated calcium release from SR. In order to lowering and maintain the calcium concentration in cytoplasmic under resting conditions, calcium are sequestered into SR by SERCA and extruded by Ca<sup>2+</sup>-Mg<sup>2+</sup>-ATPase in the plasma membrane (Landsberg and Yuan, 2004).

### 1.3.4 Potassium channels

Potassium channels control the frequency and shape of action potentials and establish cell membrane potential. This large family is classified into four groups, which are K<sub>Ca</sub>, K<sub>ATP</sub>, K<sub>V</sub>, and K<sub>IR</sub> channels. K<sub>Ca</sub> channels are activated by intracellular calcium, they consist of small-conductance (SK<sub>Ca</sub>), intermediate-conductance (IK<sub>Ca</sub>), and big-conductance calcium-activated potassium channels (BK<sub>Ca</sub>). SK<sub>Ca</sub> and IK<sub>Ca</sub> channels are more abundantly expressed in the endothelium,

but expressed poorly in the VSMCs, hence it has been claimed they are able to contribute to the endothelium-derived hyperpolarizing factor (EDHF) signals and react in the adjacent VSMCs, whereas the  $BK_{Ca}$  channels are expressed in virtually all VSMCs (Archer and Rusch, 2001, Ding et al., 2002, Eichler et al., 2003, Jakala et al., 2009, Marchenko and Sage, 1996). In VSMCs, the elevated levels of intracellular calcium cause the opening of  $BK_{Ca}$  channels which in turn allow potassium to flow out of the cell. This cause further hyperpolarization and closing of the voltage gated calcium channels (Schumacher et al., 2001).

$K_{ATP}$  channels are inhibited by intracellular ATP and are therefore likely to have a very low open probability in VSMCs under normal conditions, however the increasing intracellular cAMP levels may activate  $K_{ATP}$  channels (Sobey, 2001). The opening of these channels can cause membrane hyperpolarization and lead to vasorelaxation ( Jakala et al., 2009, Standen et al., 1989).

There are two more potassium channels which are important based on their functional roles in the regulation of membrane potential, which are  $K_V$  channels and  $K_{IR}$  channels. They are less significant when compared to  $K_{CA}$  channels and  $K_{ATP}$  channels because their functional roles are strictly regulated through the membrane potential (Loh et al., 2016).  $K_V$  channels are sensitive to voltage changes in the cell's membrane potential and serve an important buffering function against depolarization and vasoconstriction (Nelson and Quayle, 1995), whereas  $K_{IR}$  channels are activated when hyperpolarization occur, they conduct potassium current into cells and push the membrane potential back to the resting potential (Sobey, 2001).

The overall signaling pathways that mentioned above are summarized in Figure 1.2.

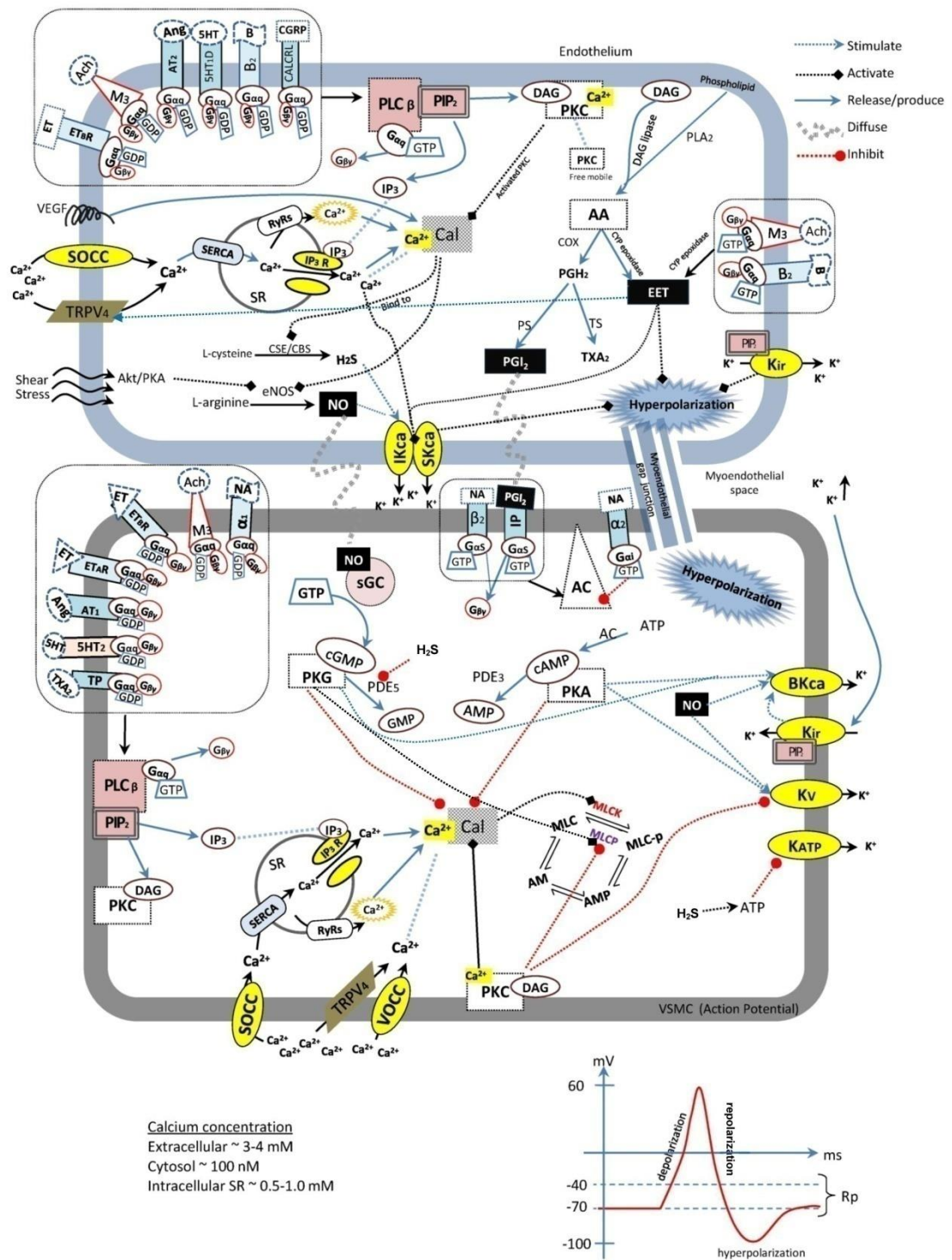


**Figure 1.2** Signaling pathways involved in vascular tone regulation.

#### 1.4 Problem statement

According to Hypertension Clinical Practice Guidelines of Malaysia, thiazide diuretics,  $\beta$ -blockers, CCBs, ACEIs, and ARBs were selected as first line monotherapy agents, but their adverse effects (constipation, dehydration, erection problem, dizziness, fatigue, joint pain, and stomach upset) and low effectivity were always being reported (Grimm et al., 1997, Husserl and Messerli, 1981, MOH, 2013). Therefore, the discovery of new drugs of employing multiple vasorelaxation-mediated signaling mechanism pathways is highly desired. Thus, the vasorelaxant effect of the potential antihypertensive herbal extracts were investigated in this study, since the extracts may contain a lot of active ingredients which can undergo multiple vasorelaxation-mediated signaling pathways and decrease the time taken to achieve the targeted blood pressure with less concomitant adverse effects.

In this study, the pharmacological activities of the above-mentioned herbal extracts (water extract, 50% ethanol extract, and 95% ethanol extract) were investigated in terms of their vasorelaxant activities through *in vitro* aortic ring assay. After that, the medicinal potential and mechanism pathways utilized by the potential herbs or extracts to induce vasorelaxant effect were also investigated through *in vitro* aortic ring assay, followed by *in vivo* antihypertensive study by oral administration to the spontaneous hypertensive rats (SHRs) for 28 days consecutively in different dosages along with toxicology study. The crude herbal extracts were expected to exert stronger vasorelaxant effect using holistic mechanism of actions compared to the monotherapy agents, as well as to exhibit a strong antihypertensive effect in *in vivo* whilst without causing adverse effect in animal models.

## 1.5 Objectives

- i. To evaluate the vasorelaxant effect of *Clinacanthus nutans* Lindau, *Strobilanthes crispus*, *Murdannia bacteata*, *Elephantopus scaber* Linn., *Pereskia bleo*, *Pereskia grandifolia* Haw., *Vernonia amygdalina*, and *Swietenia macrophylla* King seeds extracts using *in vitro* isolated rat aortic ring model.
- ii. To determine the potential extracts through *in vitro* isolated rat aortic ring model.
- iii. To investigate the mechanism actions of potential extracts using *in vitro* isolated rat aortic ring models.
- iv. To determine the antihypertensive and toxicity effects of the most potential extract in SHRs using *in vivo* model.

## CHAPTER 2

### TRI-STEP FTIR ANALYSIS OF RAW HERBS

#### 2.1 Introduction

Presently, the fingerprint of herbs or their extracts can theoretically be developed using ultraviolet (UV), thin layer chromatography (TLC), high performance liquid chromatography (HPLC), gas chromatography (GC), tandem instrumentation of liquid chromatography with mass spectrometry (LC/MS), capillary electrophoresis (CE), and deoxyribonucleic acid (DNA) chip technology (Li et al., 2010, Liang et al., 2004, Zhang et al., 2010). Nevertheless, each of them has advantages and limitations. For example, TLC is normally developed in an open system or in open condition hence results may be affected by environment factors such as humidity and temperature, which may have low reproducibility, and may be repeated only if all the factors are well standardized (Lei et al., 2010, Liang et al., 2004). Although, the above-mentioned methods can give the accurate quantity of some chemical components, but the content can only be identified with matching marker compounds (Liang et al., 2004). Furthermore, in current approaches, active or analytical markers are used for determination of specific constituents but not holistically applicable for authentication or as fingerprint. It is obviously necessary to find an analytical method that can account for thousands of components which defines the whole fingerprint of a herb or extract.

In recent years, a tri-step infrared spectroscopy method consisting of conventional Fourier transform infrared (FTIR), second derivative infrared spectroscopy (SD-IR) and two-dimensional correlation infrared spectroscopy (2D-IR)

was proposed and applied specifically for analyzing complex mixture systems (Liu et al., 2008). FTIR spectroscopy is a simple, rapid, low cost, repeatable and reproducible methodology, and is non-destructive, preserving precious samples. Moreover, various types of samples such as herbs pieces, powder, and extracts can be directly analyzed through FTIR, and the full chemical property in the analyte can be revealed and shown on FTIR spectrum. Although herbs contain large number of chemical constituents, their FTIR spectra are distinguishably different owing to the variety in the volume and variety of chemical components (Li et al., 2014).

In this study, all the collected raw herbs were identified through both biological and chemical ways. In biological way, the raw herbs were identified and authorized by a plant taxonomist, while in chemical way, the fingerprints of raw herbs were determined and characterized through tri-step FTIR method. The tri-step FTIR identification method by means of spectral resolution enhancement is used to progressively amplify the differences between the spectra in order to achieve a distinct identification of the sample. Conventional FTIR is used for a basic discrimination between the herbs and constitutes as a “primary identification”. SD-IR is used to amplify the differences obtained by using conventional FTIR spectroscopy with higher resolving power and constitutes a “secondary identification”. The 2D-IR method can obtain information on the dynamics of the sample under external perturbation and will develop the classic spectrum in the second dimension. It has a higher resolution capability and constitutes a “tertiary identification” (Sun et al., 2010).

By using the tri-step FTIR identification method, a high-quality IR spectra was obtained based on the use of the SD-IR method to increase the apparent resolution of the spectrum. The enhanced expression of sample information obtained

by using the 2D-IR method was used to distinguish between similar samples. This method was also able to verify the presence of selected components within the sample herbs.

## **2.2 Materials and methods**

### **2.2.1 Materials**

Potassium bromide (KBr) was purchased from Merck (Darmstadt, Germany).

### **2.2.2 Biological identification of herbs**

The raw aerial parts (including leaves, young stems, twigs, and flowers or fruits) of *Clinacanthus nutans* Lindau, *Strobilanthes cripus*, *Murdannia bacteata*, *Elephantopus scaber* Linn., *Pereskia bleo*, *Pereskia grandifolia* Haw., *Vernonia amygdalina*, and *Swietenia macrophylla* King were collected from the area of Paya Terubong, Penang, Malaysia and were identified by Mr. Vellosamy Shunmugam, a plant taxonomist from the School of Biological Sciences, Universiti Sains Malaysia (Zakaria et al., 2016).

After identification, the specimens for each herb were ready for preparation. Firstly the fresh aerial part of herbs were sandwiched in between newspaper sheets and dried in an oven at 38°C for one week. Next, each dried specimen was sewn onto pieces of white paper and notes about the plant was written on the lower right of the paper. After that, the specimens of *C. nutans*, *S. cripus*, *M. bacteata*, *E. scaber*, *P. bleo*, *P. grandifolia*, *V. amygdalina*, and *S. macrophylla* were authenticated by Dr. Rahmad Zakaria and the voucher specimens of these herbs with the references no. of 11700, 11701, 11702, 11703, 11704, 11705, 11706, and 11707, respectively were



deposited in the Herbarium of the School of Biological Sciences, USM (Appendix A – H).

### 2.2.3 Tri-step FTIR identification method

A spectrum 400 FTIR spectrometer (Perkin-Elmer) equipped with a Deuterated Tri-Glycine Sulfate (DTGS) detector was used to characterize the herbs. A tablet of KBr was used as the background. The dried leaves of *C. nutans*, *S. cripus*, *M. bacteata*, *E. scaber*, *P. bleo*, *P. grandifolia*, *V. amygdalina*, and dried seeds of *S. macrophylla* were pulverized and passed through a 200-mesh sieve. Each sample powder (about 1 – 2 mg) was mixed evenly with 100 mg of crystalline KBr. The mixture was ground and pressed into a tablet at a pressure of not more than 10 psi for two minutes. After that, the spectra were calculated from a total of 16 co-added scans in the range of 400 – 4000  $\text{cm}^{-1}$  with a resolution of 4  $\text{cm}^{-1}$ . The interferences of water and carbon dioxide were eliminated online when scanning. The raw FTIR data were then processed by using the spectrum software of the Perkin-Elmer FTIR spectrometer (version 6.3.5). The FTIR spectrum was generally accepted when a transmission higher than 60% was achieved. Otherwise, the test was repeated with either the sample powder or KBr added (Choong et al., 2014).

All the SD-IR spectra were obtained after Savitzky-Golay polynomial fitting (13-point smoothing) of the original IR spectra taken at room temperature. To obtain the 2D-IR spectrum, the sample tablet was placed into the sample pool with a programmable heated jacket controller (Model GS20730, Specac). In order to avoid the loss of or change in some of the unstable compositions, the dynamic spectra were collected at different temperatures ranging from room temperature to 120°C at intervals of  $10 \pm 2^\circ\text{C}$  (with a rate of increase of  $2^\circ\text{C}/\text{min}$ ). The full temperature scan

took a total time of 50 minutes for each sample. Then, the 2D-IR correlation spectra were obtained by treating the series of dynamic spectra with the 2D-IR correlation analysis software developed by Tsinghua University, Beijing, China (Li et al., 2014, Li et al., 2010).

## **2.3 Results and discussion**

The conventional FTIR spectra of the herbs are shown in Figure 2.1, and their characteristic absorption peaks are assigned in Table 2.1. Their SD-IR spectra and 2D-IR spectra are shown in Figure 2.2 and Figure 2.3, respectively.

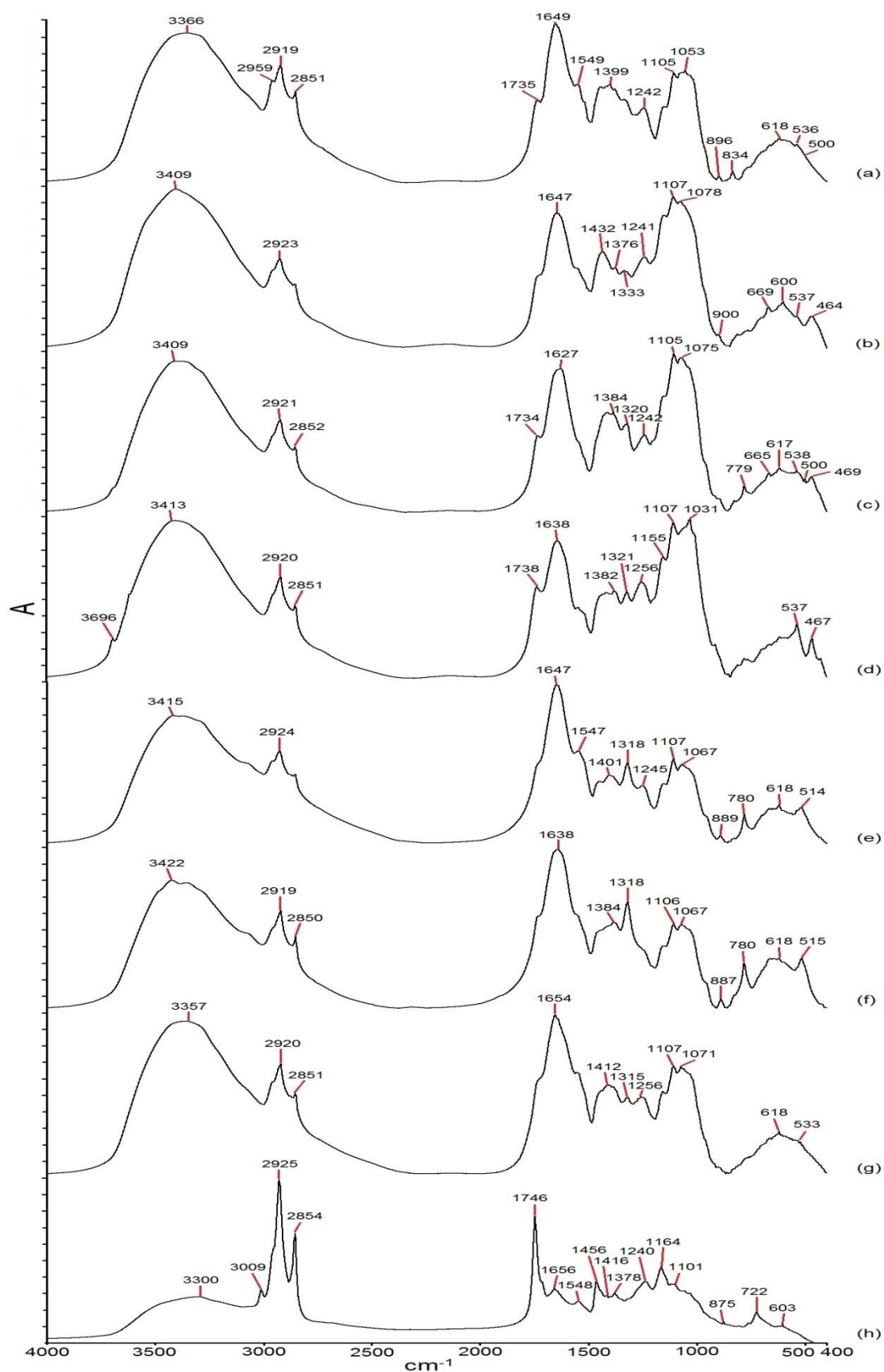
### **2.3.1 Assignments and comparison by using conventional FTIR spectra**

Figure 2.1 shows the conventional FTIR spectra of the leaves of *C. nutans*, *S. cripus*, *M. bacteata*, *E. scaber*, *P. bleo*, *P. grandifolia*, *V. amygdalina*, and seeds of *S. macrophylla*. The peaks that appeared at  $3400 - 3300\text{ cm}^{-1}$  are O-H stretching vibration absorption peaks. The peaks nearby at  $2921\text{ cm}^{-1}$  and  $2851\text{ cm}^{-1}$ , are methylene C-H asymmetric and symmetric stretching vibration absorption peaks, respectively. The peak at  $1735\text{ cm}^{-1}$  is the carbonyl group C=O stretching vibration absorption peak. The peaks nearby at  $1640\text{ cm}^{-1}$  contain O-H bending vibration absorption and conjugated carbonyl stretching vibration absorption peaks. The absorption peaks within the  $1430 - 1400\text{ cm}^{-1}$  region contain a variety of ingredients, such as C-H bending vibration absorption and (O)C-H stretching vibration peaks, while the peaks in the range of  $1300 - 950\text{ cm}^{-1}$  are the absorption peaks for all types of C-O stretching (see Table 2.1).

In Figure 2.1, all the spectra of the herbs, except that for *S. macrophylla* seed, are very similar. An obvious difference between them lies in the intensities of the absorption peaks in the range of  $1200 - 950\text{ cm}^{-1}$ , corresponding to the peak intensity nearby at  $1640\text{ cm}^{-1}$ . The absorption peaks of *S. cripus*, *M. bacteata*, and *E. scaber* (Figure 2.1b, 2.1c, and 2.1d) in the range of  $1200 - 950\text{ cm}^{-1}$  have higher intensities than the absorption peaks at  $1640\text{ cm}^{-1}$ , in contrast to the peak intensities of other herbs. This indicates that *S. cripus*, *M. bacteata*, and *E. scaber* have a higher content of saccharides or sugar than the other herbs. In the spectra of *C. nutans* and *P. bleo* (Figure 2.1a and 2.1e), both the  $1649\text{ cm}^{-1}$  and  $1549\text{ cm}^{-1}$  absorption peaks appears simultaneously in their spectra. The shapes of these two absorption peaks correspond to those of the amide I and amide II proteins, indicating that these two herbs contain a certain amount of protein. In addition, the spectra of *P. bleo* and *P. grandifolia* (Figure 2.1e and 2.1f) record the appearance of some absorption peaks at  $1318\text{ cm}^{-1}$ ,  $780\text{ cm}^{-1}$ , and  $514(515)\text{ cm}^{-1}$ , which are due to the symmetrical stretching vibration and bending vibration absorption of the C-O bond of oxalate ions. This indicates that *P. bleo* and *P. grandifolia* contain a certain amount of calcium oxalate.

The spectrum of *S. macrophylla* seed is completely different from the spectra of the other herbs. This is because seed has higher content of plant oil and show obvious characteristic peaks in its IR spectrum. The molecule of oil is a long-chain fatty acid ester. The main functional groups contained in the oil are a methylene group and an ester carbonyl. The spectrum of *S. macrophylla* seed (Figure 2.1h) shows more C=C double bonds due to the fact that the plant oil contains more unsaturated fatty acid. Therefore, a significant alkene C-H stretching absorption peak ( $3009\text{ cm}^{-1}$ ) is observed in its spectrum. The peak at  $2925\text{ cm}^{-1}$  is the absorption peak due to the methylene C-H asymmetric stretching vibration, and the peak at  $2854\text{ cm}^{-1}$

is the absorption peak due to the methylene C-H symmetric stretching vibration. In addition, the peak at  $1746\text{ cm}^{-1}$  is the absorption peak for the ester carbonyl C=O stretching vibration while the peak appearing at  $722\text{ cm}^{-1}$  (C-H bending vibration) indicates that *S. macrophylla* seed contains long-chain carbons ( $^n\text{C} > 4$ ).



**Figure 2.1** Conventional FTIR spectra of (a) *C. nutans*, (b) *S. crispus*, (c) *M. bacteata*, (d) *E. scaber*, (e) *P. bleo*, (f) *P. grandifolia*, (g) *V. amygdalina*, and (h) *S. macrophylla* seed. Notes: A, absorbance

**Table2.1** Peak assignments on the conventional FTIR spectra of herbs

Peak (cm <sup>-1</sup> )								Primary assignment	Possible compounds
<i>C. nutans</i>	<i>S. crispus</i>	<i>M. bracteata</i>	<i>E. scaber</i>	<i>P. bleo</i>	<i>P. grandifolia</i>	<i>V. amygdalina</i>	<i>S. macrophylla</i>		
-	-	-	3696	-	-	-	-	O-H, $\nu$	Various
3366	3409	3409	3413	3415	3422	3357	3300	O-H, $\nu$	Various
-	-	-	-	-	-	-	3009	C-H, $\nu$	Alkene
2959	-	-	-	-	-	-	-	C-H, $\nu_{as}$	Various
2919	2923	2921	2920	2924	2919	2920	2925	C-H, $\nu_{as}$	Various
2851	-	2852	2851	-	2850	2851	2854	C-H, $\nu_s$	Various
1735	1734	1738	-	-	-	-	1746	C=O, $\nu$	Ester
1649	-	-	-	1647	-	-	1656	N-H, $\delta$	Amide I
-	1647	1627	1638	-	1638	1654	-	O-H, $\delta$	Saccharides
1549	-	-	-	1547	-	-	1548	N-H, $\delta$	Amide II
-	-	-	-	-	-	-	1465	Ring	Aromatic
-	1432	-	-	-	-	1412	1416	C-H, $\delta$	Saccharides
1399	-	-	-	1401	-	-	-	(O) C-H, $\nu$	Saccharides
-	1376	1384	1382	-	1384	-	1378	(O) C-H, $\delta$	Ester
-	1333	1320	1321	-	-	1315	-	(O) C-H, $\delta$	Saccharides
-	-	-	-	1318	1318	-	-	C-O, $\nu_s$	Calcium oxalate
1242	1241	1242	1256	1245	-	1256	1240	C-O, $\nu$	Ester, Glycoside
-	-	-	1155	-	-	-	1164	C-O, $\nu$	Saccharides
1105	1107	1105	1107	1107	1106	1107	1101	C-O, $\nu$	Saccharides
1053	1078	1075	1031	1067	1067	1071	-	C-O, $\nu$	Saccharides

Notes:  $\nu$ , stretching;  $\nu_s$ , symmetrical stretching;  $\nu_{as}$ , asymmetrical stretching;  $\delta$ , bending.

### 2.3.2 Comparison and discussion of the SD-IR spectra

The SD-IR spectra can resolve the problem of overlapping peaks, enhance the spectral characteristics, and improve the apparent resolution in the IR spectrum. Figure 2.2 shows the SD-IR spectra of the herbs within the wave-number range of  $1800 - 800 \text{ cm}^{-1}$ , which contains the main absorption bands of the chemical constituents of the herbs. As shown in the figure, some relatively weak absorption peaks in the conventional IR spectra can be seen more clearly in the SD-IR spectra (Sun et al., 2010).

In Figure 2.2, the intensities of the peak around  $1740 \text{ cm}^{-1}$  (carbonyl C=O stretching vibration) among these eight herbs are not the same. The strongest peak is from *S. macrophylla* seed (Figure 2.2h), indicating that it has the highest content of ester compounds. The appearance of the absorption peaks at 1165, 1078, 989, 952, 890, and  $826 \text{ cm}^{-1}$  in the spectrum of *M. bacteata* (Figure 2.2c) can be ascribed to the herb contains more stachyose. In the SD-IR spectra of *P. bleo* and *P. grandifolia* (Figure 2.2e and 2.2f), the absorption peaks at  $1317 \text{ cm}^{-1}$  are very strong, once again showing that they have a high content of calcium oxalate.

In the SD-IR spectrum of *C. nutans* (Figure 2.2a), the absorption peaks at 1739, 1715, 1635 (C=O stretching vibration), 1577, 1540, 1516, 1496 (aromatic ring skeleton vibration), 1472, 1375 (C-H bending vibration), and  $1282 \text{ cm}^{-1}$  (C-O stretching vibration) are stronger, which indicates that it contains more flavonoids. *S. crispus*, *V. amygdalina*, and *S. macrophylla* seed (Figure 2.2b, 2.2g, and 2.2h) also have absorption peaks due to C=O stretching (around  $1740 \text{ cm}^{-1}$  and  $1660 \text{ cm}^{-1}$ ), aromatic ring skeleton vibration (around  $1545 \text{ cm}^{-1}$ ), and C-H bending vibration (around  $1470 \text{ cm}^{-1}$ ) in their spectra; therefore, they also contain flavonoids. The